# Catalysis Science & Technology

Accepted Manuscript

Volume 1 | Number 1 | Jan 2013 | Pages 1–100

Catalysis Science & Technology

www.rsc.org/catalysis

ROYAL SOCIETY OF CHEMISTRY

ROYAL SOCIETY OF CHEMISTRY

www.rsc.org/catalysis

Journal Name

ARTICLE

# Copper Supported on $H^+$-Modified Manganese Oxide Octahedral Molecular Sieves (Cu/H-OMS-2) as a Heterogeneous Biomimetic Catalyst for the Synthesis of 3-Aroylimidazopyridines and 3-Aroylimidazopyrimidines

eceived 00th January 20xx,
Accepted 00th January 20xx

DOI: 10.1039/x0xx00000x

www.rsc.org/

Xu Meng,[a] Jinqi Zhang,[a] Baohua Chen,[b] Zhenqiang Jing[c] and Peiqing Zhao*[a]

Copper supported on acid-modified manganese oxide octahedral molecular sieves (Cu/H-OMS-2) was prepared and found to be a versatile catalyst for the oxidative synthesis of 3-aroylimidazopyridines with a broad substrate scope. Cu/H-OMS-2 that was characterized by BET, XRD, XPS, FTIR, TEM, SEM, $H_2$-TPR and $O_2$-TPD techniques could also be used to synthesize 3-aroylimidazopyrimidines and applied in one-pot, three-component reactions of ketones, aldehydes and 2-aminopyridines. The catalytic system employs low loading Cu as the catalytic metal and support H-OMS-2 as the electron-transfer mediator (ETM) to sequentially lower the redox energy barrier, which generates a low-energy pathway and enables the reaction to proceed in a biomimetic way. Moreover, Cu/H-OMS-2 could be reutilized for 4 times with a slight decrease in the catalytic activity.

## Introduction

Within the past decades, OMS-2, microporous tunnel-structured manganese oxide octahedral molecular sieves, has attracted great interest in catalysis, materials and environmental science.[1] In particular, OMS-2 has been treated as a versatile redox catalyst in various oxidations because it has superior properties, such as excellent structural stability, mixed valence, large surface areas, electron-conducting properties and oxygen reduction abilities.[2,3] Meanwhile, modified OMS-2 via ion-exchange has also been prepared and applied in oxidations.[4] Moreover, OMS-2 has been employed as a support of the supported catalysts in heterogeneous catalysis, which was fruitfully used to CO oxidation,[5] VOCs combustion[6] and removal of HCBz.[7] Therefore, developing useful and sustainable catalytic systems by the use of OMS-2 is desirable and challenging.

From the perspective of redox potential, mixed valent OMS-2 that works as a support and an electron-transfer mediator (ETM)[8] at the same time can interact with the supported catalytic metal (M) to lower the energy barrier of an oxidation in theory as long as the redox potential of OMS-2 is between the potential of $M_{red}/M_{ox}$ and green oxidant $O_2/H_2O$ (Scheme 1).[9] In this way, electrons of an oxidative transformation can rapidly transfer from the substrate to the oxidant in a biomimetic way by the use of ETM, which enhances the catalytic efficiency, lowers the catalytic metal loading, enables $O_2$ to be an efficient oxidant and produces water as the sole byproduct. On the basis of this strategy, we previously developed a heterogeneous biomimetic $CuO_x$/OMS-2-catalyzed synthesis of 3-iodoimidazopyridines using air as the oxidant under a low-energy pathway.[9a] Likewise, Mizuno`s group previously reported a biomimetic homocoupling of alkynes catalyzed by $Cu(OH)_x$/OMS-2.[9b] Our continued interest in this field prompts us to discover other efficient and novel OMS-2-based catalytic systems that are able to sequentially decrease the redox energy barriers in oxidative transformations.

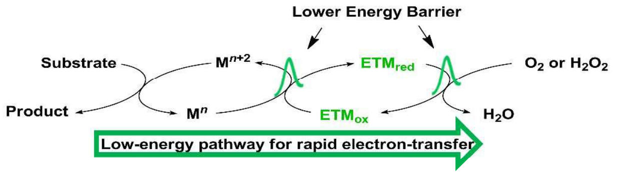

**Scheme 1** The oxidations involve the use of ETM under a long-energy pathway.

Imidazo[1,2-*a*]pyridines are very important structural motifs and have been found in various biologically active and pharmaceutical compounds because they are antiviral, antimicrobial, antitumour, anti-inflamatory, antiparasitic, hypnotic, etc..[10] Many commercial drugs involve imidazopyridines, like zolpidem, zolimidine, alpidem, saripidem and necopidem.[11] Especially, 3-aroylimidazo[1,2-*a*]pyridines exhibit excellent anticancer property.[12] The most

---

[a] State Key Laboratory for Oxo Synthesis and Selective Oxidation, Suzhou Research Institute of LICP, Lanzhou Institute of Chemical Physics (LICP), Chinese Academy of Sciences, Lanzhou 730000, China. Fax: + 96 931 8277008; Tel: + 86 931 4968688; E-mail: zhaopq@licp.cas.cn
[b] State Key Laboratory of Applied Organic Chemistry, Lanzhou University, Lanzhou, 730000, China
[c] Suzhou Institute of Nano-Tech and Nano-Bionic (SINANO), Chinese Academy of Sciences, Suzhou 215123, China

† Electronic Supplementary Information (ESI) available: [Experimental details, spectra data of the products and copies of spectra]. See DOI: 10.1039/b000000x/

traditional method of obtaining 3-aroylimidazo[1,2-*a*]pyridines is functionalization of imidazo[1,2-*a*]pyridines by three steps, including formylation, Grignard reaction and oxidation.[12a] Most recently, homogeneous Cu-catalyzed oxidative cyclizations for the synthesis of 3-aroylimidazo[1,2-*a*]pyridines from chalcones and 2-aminopyridines via C-N bond-forming were developed.[13] Nevertheless, the aforementioned homogeneous catalysis generally produces a little of byproducts, like Michael adducts and another cyclized product naphthyridines,[14] because of high level of activity derived from its uniformity on a molecular level and solubility in the reaction medium. In addition, the separation, recovery and recycling of catalysts is relatively hard to achieve in homogeneous reactions.[15] So, there is an incentive to develop a heterogeneous process able to produce 3-aroylimidazo[1,2-*a*]pyridines by an environmentally friendly concept while minimizing the byproducts and wastes.

As a part of our continuing efforts on developing efficient heterogeneous catalytic systems and their applications in organic transformations,[3e,9a] we now present the study of immobilized copper on $H^+$-modified OMS-2 as a catalyst (Cu/H-OMS-2) that can sequentially decrease the energy barrier of the oxidation and generate a low-energy pathway in the synthesis of 3-aroylimidazo[1,2-*a*]pyridines under air (Scheme 2). The heterogeneous system can also tolerate 2-aminopyrimidine as a substrate and offer 3-aroylimidazo[1,2-*a*]pyrimidines in good yields. Furthermore, the desired heterocycles can be obtained *via* one-pot, three-component reactions of aldehydes, ketones and aminopyridines using Cu/H-OMS-2.

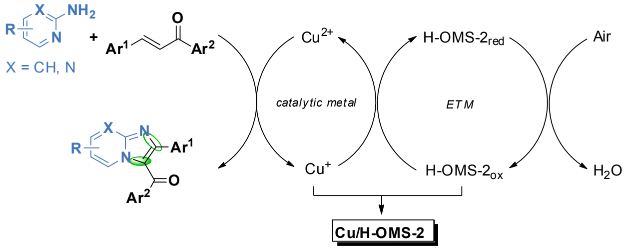

**Scheme 2** Cu-catalyzed multistep oxidation using H-OMS-2 as an ETM for the synthesis of imidazo[1,2-*a*]pyridines and imidazo[1,2-*a*]pyrimidines.

## Results and Discussion

Cu/H-OMS-2 was prepared *via* wet-impregnation using $Cu(NO_3)_2{\cdot}3H_2O$ as the copper precursor in deionized water. Elemental analysis of the catalyst by atomic absorption spectrometry (AAS) showed the quantities of Cu in the sample was 1.58 wt.%. The BET surface areas and porosities of Cu/H-OMS-2 were determined by $N_2$ adsorption−desorption at 77 K and the results showed that the BET surface area is 87 $m^2/g$, pore volume is 0.4 $cm^3/g$ and pore size is 136 Å. X-ray diffraction (XRD) was employed to characterize OMS-2, H-OMS-2 and Cu/H-OMS-2 respectively (Fig. 1, left). XRD patterns showed the diffraction peaks of H-OMS-2 and Cu/H-OMS-2 were the same as that of OMS-2, which means Cu/H-OMS-2 and its support both are typical cryptomelane materials (JCPDS file #29-1020). No signals due to copper metal (cluster) or copper oxide were observed, which indicates that the copper oxide was low loading and highly dispersed on H-OMS-2. Notably, the diffraction peaks of Cu/H-OMS-2 and H-OMS-2 became slightly narrower and sharper compared with OMS-2, which suggests the crystallite sizes of them increased. The lattice vibrational behaviour of the Cu/H-OMS-2 was studied by FTIR spectroscope to detect the effect of Cu and $H^+$ substitution on the spectral features of OMS-2. As shown in Fig. 1 (right), we obtained similar IR spectra from OMS-2, H-OMS-2 and Cu/H-OMS-2 respectively. All samples displayed four characteristic bonds at 714 $cm^{-1}$, 606 $cm^{-1}$, 521 $cm^{-1}$ and 465 $cm^{-1}$ with comparable relative intensities that can be corresponded to Mn-O lattice vibration modes in $MnO_6$ octahedra.[4d] Additionally, TEM images showed H-OMS-2 and Cu/H-OMS-2 (for SEM image, see SI, Figure S1) have a typical nano-rod morphology,[4] which means the acid-modification and the supported copper do not change the structure of OMS-2 (Figure 2).

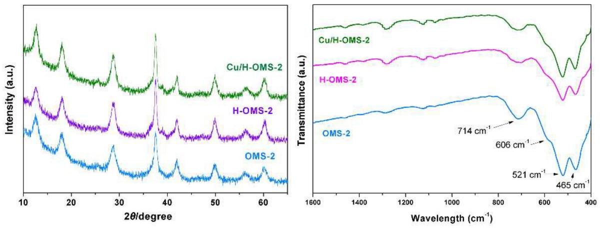

**Figure 1** XRD (left) and IR spectra (right) of OMS-2, H-OMS-2 and Cu/H-OMS-2.

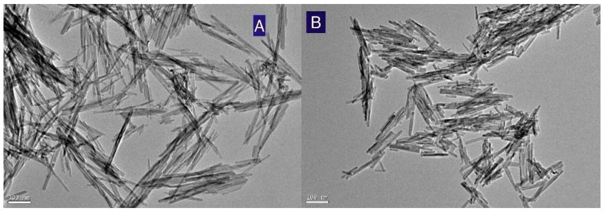

**Figure 2** TEM images of H-OMS-2 (A) and CuO/H-OMS-2 (B).

The redox ability of Cu/H-OMS-2 was measured by the means of $H_2$-TPR, while support H-OMS-2 and OMS-2 were also examined for comparison. For all OMS-2-based materials, the reduction of $MnO_2$ to MnO proceeds in two different steps ($MnO_2$ to $Mn_3O_4$ to MnO) generally, but these processes overlap sometimes.[5a] As shown in Fig. 5, the overlapping peaks (a) from 369 °C to 395 °C are ascribed to the reduction of $MnO_2$ to MnO of OMS-2. For H-OMS-2, the two reduction peaks (b and b') of $MnO_2$ which were demonstrated at 345 °C and 387 °C shifted to lower temperatures, suggesting the reducibility of H-OMS-2 was improved by $H^+$-modification. Furthermore, two new peaks (α and β) appeared at the temperature range of 250-300 °C, which are ascribed to the partial reduction of $MnO_2$ species derived from the interaction between $H^+$ and $MnO_2$.[5a] Specifically, α peak probably corresponds to the reduction of $MnO_6$-□ (□ stands for oxygen vacancies) and the β peak likely corresponds to the reduction of $MnO_6$-$K^+$ and $MnO_6$-$H^+$. For Cu/H-OMS-2, four reduction peaks (c, c`, α` and β`) all shifted to lower temperatures compared with its support H-OMS-2 and OMS-2, implying the further enhanced redox ability. In particular, α` peak generally corresponds not only to the reduction of well-dispersed CuO particles but also to the partial reduction of $MnO_2$ species. The improved reduction of $MnO_2$ is due to the spillover hydrogen from copper atoms to manganese oxides. It is believed that β` peak corresponds to the combined reduction of large CuO particles and $MnO_2$.[5a] Cu/H-OMS-2 has lager α` and β` peaks and more obvious c and c` peaks, which probably indicates $Cu^{2+}$-O-$Mn^{4+}$ entities were formed at the interface between CuO and H-OMS-2 and the mobility of oxygen was promoted by electronic delocalization effect between Cu and Mn species.[5b,7] Furthermore, the XPS of Mn 2p from H-OMS-2 and Cu/H-OMS-2 also indicates that there is an interaction between copper and H-OMS-2 (for detailed discussion, see ESI, Fig. S2). The phenomenon of electron transfer between the catalytic metal copper and the electron-transfer mediator H-OMS-2 probably can be proved from these observations.

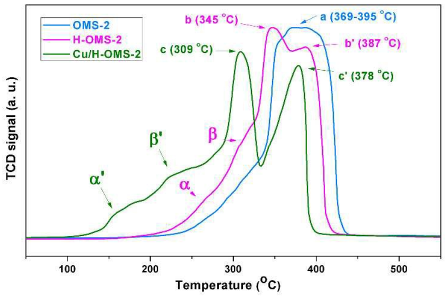

**Figure 3** $H_2$-TPR of OMS-2, H-OMS-2 and Cu/H-OMS-2.

Then, $O_2$-TPD technology was used to analyze the oxygen species of Cu/H-OMS-2. As shown in Fig. S3 (see SI), the very similar peaks from desorption of H-OMS-2 and Cu/H-OMS-2 were obtained, and the majority of oxygen species can be corresponded to lattice oxygen.[7] Specifically, the similar and clear shoulder peaks at around 500 °C can be ascribed to surface oxygen species or the labile oxygen species. The peaks at around 600 °C and 750 °C result from the transformation of cryptomelane to $Mn_2O_3$ and further to $Mn_3O_4$.[4e] Oxygen atoms in the framework bound to Mn(III) have a weaker interaction compared with the interaction between oxygen atoms and Mn(IV), so two different oxygen species were released at middle temperature and high temperature respectively during TPD.

The oxidative cyclization between 2-aminopyridine and chalcone was selected as a model reaction to test the catalytic activity of Cu/H-OMS-2 (Table 1). From a synthetic point of view, the copper-catalyzed cyclization of **1a** and **2a** will lead to 3-aroylimidazo[1,2-*a*]pyridine as the desired product with **3aa** and another product naphthyridine which comes from a competitive cyclization as byproducts.[14] Michael adduct **3aa** actually is the intermediate during the formation of **3a**, which means the high yield of **3a** depends on the efficient formation of **3aa** firstly and the subsequent intermolecular oxidative cyclization of it. So, we screened different parameters, such as the catalyst, the solvent and the temperature, to determine the best catalytic system for obtaining high yield of 3-aroylimidazo[1,2-*a*]pyridine. In the initial experiment, OMS-2 was treated with reactants in DCB at 80 °C under air for 20 h, which did not show any catalytic activity (Table 1, entry 1). When we switched the catalyst to Cu/OMS-2 under the same conditions, **3a** and **3aa** were both obtained in low yields (Table 1, entry 2). However, the formation of **3a** failed o proceed using $Cu(OH)_x$/OMS-2 as a catalyst (Table 1, entry 3). An attempt to employ Cu/H-OMS-2 (12 mg, 0.7 mol%, Cu: 1.58 wt.%) in the synthesis of 3-aroylimidazo[1,2-*a*]pyridine was also unfruitful, and **3a** was produced in 10% yield with 18% yield of **3aa** (Table 1, entry 4). To our delight, increasing the reaction temperature to 100 °C enhanced the yield of **3a** to 23% with a trace amount of **3aa** when Cu/H-OMS-2 was used as a catalyst (Table 1, entry 5). Next, a lot of solvents were examined to further better the yield of **3a** at 100 °C with Cu/H-OMS-2 (Table 1, entries 6-10). It was found that apolar $Cl_2CHCHCl_2$ gave the highest yield of **3a** (41%) in the absence of byproducts and HOAc provided 0% yield of **3a** but 59% yield of **3aa** within 3 h in the presence of Cu/H-OMS-2 (Table 1, entries 9 and 10). Therefore, we envisioned that the mixed solvent of HOAc and $Cl_2CHCHCl_2$ probably could efficiently transform **3aa** and give **3a** in high yield because HOAc is suited for the generation of Michael adduct **3aa** and able to enhance the

**Table 1** Optimization of reaction conditions[a]

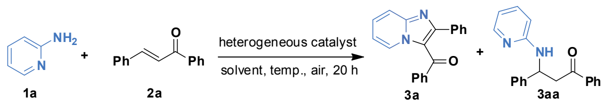

| Entry | Catalyst | Solvent | *T* [°C] | Yield[b] (%) **3a** | **3aa** |
|---|---|---|---|---|---|
| 1 | OMS-2 | DCB | 80 | 0 | 0 |
| 2[c] | Cu/OMS-2 | DCB | 80 | 15 | 28 |
| 3[d] | $Cu(OH)_x$/OMS-2 | DCB | 80 | 0 | <5 |
| 4 | Cu/H-OMS-2 | DCB | 80 | 10 | 18 |
| 5 | Cu/H-OMS-2 | DCB | 100 | 23 | <5 |
| 6 | Cu/H-OMS-2 | DMSO | 100 | 8 | 12 |
| 7 | Cu/H-OMS-2 | $MeNO_2$ | 100 | 8 | <5 |
| 8 | Cu/H-OMS-2 | Toluene | 100 | 13 | 25 |
| 9[e] | Cu/H-OMS-2 | HOAc | 100 | 0 | 59 |
| 10 | Cu/H-OMS-2 | $Cl_2CHCHCl_2$ | 100 | 41 | 0 |
| *11*[f] | *Cu/H-OMS-2* | *$Cl_2CHCHCl_2$/HOAc* | *100* | *89* | *0* |
| 12[f] | Cu/H-OMS-2 | Xylene/HOAc | 100 | 12 | 0 |
| 13[f] | Cu/H-OMS-2 | Dioxane/HOAc | 100 | 10 | 0 |
| 14[f] | Cu/H-OMS-2 | DMF/HOAc | 100 | <5 | 0 |
| 15[f, g] | Cu/H-OMS-2 | $Cl_2CHCHCl_2$/HOAc | 100 | 42 | 16 |
| 16[f] | Cu/H-OMS-2 | $Cl_2CHCHCl_2$/HOAc | 70 | 0 | 0 |
| 17[f] | Cu/H-OMS-2 | $Cl_2CHCHCl_2$/HOAc | 120 | 76 | 0 |
| 18[f, h] | CuO + H-OMS-2 | $Cl_2CHCHCl_2$/HOAc | 100 | <5 | 40 |
| 19[f,i] | CuO | $Cl_2CHCHCl_2$/HOAc | 100 | <5 | 45 |

[a] Reaction conditions: **1a** (0.6 mmol), **2a** (0.4 mmol), catalyst (12 mg), solvent (1.2 mL), air, 20 h. [b] Isolated yields. [c] 12 mg of Cu/OMS-2 (Cu: 1.65 wt%) was used. [d] 12 mg of $Cu(OH)_x$/OMS-2 (Cu: 1.45 wt%) was used. [e] For 3 h. [f] 0.1 mL of HOAc was used to comprise the mixed solvent. [g] Under $O_2$. [h] 1 mol% of CuO and 12 mg H-OMS-2 were used. [i] 0.4 mmol of CuO was used.

electrophilic ability of copper while $Cl_2CHCHCl_2$ is superior for the oxidative cyclization. As expected, when we added 0.1 mL of HOAc into 1.2 mL $Cl_2CHCHCl_2$ as a mixed solvent in the reaction, the desired product **3a** was obtained in 89% yield without **3aa** and other byproducts (Table 1, entry 11). Subsequently, a series of mixed solvents containing HOAc were investigated, but the results were not satisfied (Table 1, entries 12-14). Performing the reaction under $O_2$ also slashed the reaction (Table 1, entry 15). Next, the reaction temperature was changed and the results demonstrated that the reaction did not proceed below 80 $^{o}$C and higher temperature did not improve the reaction (Table 1, entries 16 and 17). Finally, control experiments of the catalysts were run in the mixed solvent under air at 100 $^{o}$C. The physical mixture of bulk CuO and H-OMS-2 only gave Michael adduct **3aa** as the main product, while **3a** was barely observed by the use of stoichiometric amount of bulk CuO in the reaction (Table 1, entries 18 and 19). These observations suggest that the highly dispersed copper species on H-OMS-2 play a key role in the oxidative cyclization and there is an interaction between supported copper and H-OMS-2. As a result of the optimization, we concluded that the best reaction conditions to cyclization of 2-aminopyridine and chalcone in a mixed solvent of $Cl_2CHCHCl_2$/HOAc involve the use of Cu/H-OMS-2 as the catalyst at 100 $^{o}$C for 20 h with air as the oxidant.

**Table 2** Synthesis of 3-aroylimidazo[1,2-*a*]pyridines catalyzed by Cu/H-OMS-2[a]

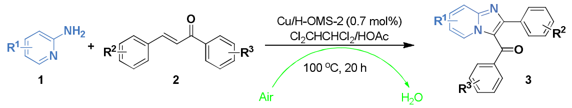

| Product | $R^1$ | $R^2$ | $R^3$ | Yield (%)[b] |
|---|---|---|---|---|
| **3b** | H | 4-Cl | H | 76 |
| **3c** | H | 4-Cl | 4-Cl | 82 |
| **3d** | H | H | 4-Cl | 88 |
| **3e** | H | 2-Cl | H | <5 |
| **3f** | H | 4-OMe | H | 79 |
| **3g** | H | H | 4-OMe | 65 |
| **3h** | H | H | 3,4-diOMe | 45 |
| **3i** | H | 4-$NO_2$ | H | 84 |
| **3j** | H | 4-F | 4-Me | 60 |
| **3k** | 3-Me | H | H | 72 |
| **3l** | 3-Me | 4-Cl | 4-Cl | 71 |
| **3m** | 4-Me | 2-Cl | H | <5 |
| **3n** | 4-Me | 4-Cl | 4-Cl | 70 |
| **3o** | 5-Me | H | H | 66 |
| **3p** | 5-Me | 4-Cl | 4-Cl | 64 |
| **3q** | 5-Me | H | 4-Cl | 69 |
| **3r** | 5-Me | 4-F | 4-Me | 53 |
| **3s** | 4-$CF_3$ | 4-Cl | 4-Cl | 39 |
| **3t** | 3-Br | 4-Cl | 4-Cl | 45 |
| **3u** | 5-Br | 4-Cl | 4-Cl | 42 |
| **3v** | 4-Cl | 4-Cl | 4-Cl | 55 |
| **3w** | 5-Cl | 4-Cl | 4-Cl | 52 |
| - | 5-COOMe | H | H | 0 |
| - | 3-CN | H | H | 0 |

[a] Reaction conditions: **1** (0.6 mmol), **2** (0.4 mmol), Cu/H-OMS-2 (12 mg, 0.7 mol%), $Cl_2CHCHCl_2$ (1.2 mL), HOAc (0.1 mL), 100 $^{o}$C, 20 h, air. [b] Isolated yields.

With the optimized conditions in hand, we investigated the substrate scope of the cyclization (Table 2). Firstly, various substituted chalcones were tolerable in the reactions and gave corresponding 3-aroylimidazo[1,2-*a*]pyridines in moderate to good yields (Table 2, **3a**-**3j**). The Michael adduct byproducts were not observed in all cases. Generally, chalcones with electron-withdrawing substitutes offered higher yields of desired products than electron-rich chalcones did. Sterically hindered chalcone, like 2-chlorochalcone, did not proceed in the reaction (Table 2, **3e**). On the other hand, a number of substituted 2-aminopyridines smoothly participated in the reactions and provided desired products in good yields without the observation of Michael adducts. Specifically, 2-aminopyridines with electron-donating groups showed higher activity in comparison with ones with electron-withdrawing groups, such as halogens (Table 2, **3k**-**3w**). More importantly, many multi-halogen-substituted 3-aroylimidazo[1,2-*a*]pyridines were obtained in 42-64% yields, which provides opportunities to further functionalize these halogen-substituted products using coupling techniques.[18] Nevertheless, 2-aminopyridines with sensitive groups, like -COOMe and -CN, failed to proceed under the present system because HOAc of the solvent decomposed these substrates quickly.

**Table 3** Synthesis of 3-aroylimidazo[1,2-*a*]pyrimidines catalyzed by Cu/H-OMS-2[a]

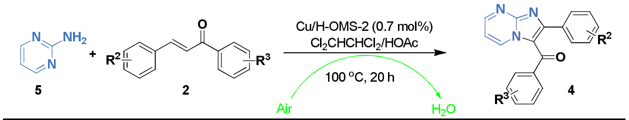

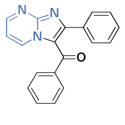
**4a**, 76%

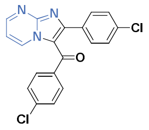
**4b**, 82%

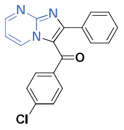
**4c**, 81%

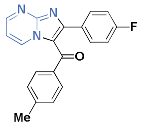
**4d**, 46%

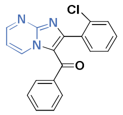
**4e**, 25%

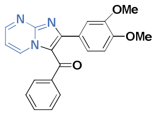
N.R.

[a] Reaction conditions: **5** (0.6 mmol), **2** (0.4 mmol), Cu/H-OMS-2 (12 mg, 0.7 mol%), $Cl_2CHCHCl_2$ (1.2 mL), HOAc (0.1 mL), 100 $^{o}$C, 20 h, air, isolated yields.

In order to further study the generality of this heterogeneous process, 2-aminopyrimidine **5** was used as a substrate to synthesize 3-aroylimidazo[1,2-*a*]pyrimidines. Gratifyingly, 2-aminopyrimidine worked very well with chalcones and good yields of 3-aroylimidazo[1,2-*a*]pyrimidines **4a-4d** were obtained fruitfully (Table 3). To the best of our knowledge, this is the first example that heterogeneous copper-based material catalyzed the synthesis of 3-aroylimidazo[1,2-*a*]pyrimidines between 2-aminopyrimidine and chalcones *via* oxidative C-N bond-forming.[13d] However, steric hindrance affected the reactions significantly (Table 3, **4e**) and electron-rich substrate, dimethoxychalcone, did not participate in the reaction at all. Unfortunately, 2-aminopyrazine and 2-aminothiazole were not tolerant under the present catalytic system.

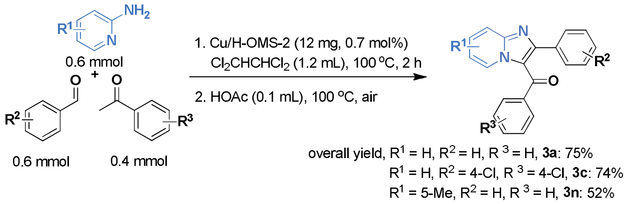

**Scheme 3** One-pot synthesis of 3-aroylimidazo[1,2-*a*]pyridines from ketone, aldehyde and 2-aminopyridine.

From a synthetic point of view, to make this heterogeneous approach to 3-aroylimidazo[1,2-*a*]pyridines more attractive, we investigated their formation *via* a one-pot, three-component reaction sequence that avoids to isolate the chalcone intermediate. In $Cl_2CHCHCl_2$, acetophenone reacted with aldehyde catalyzed by Cu/H-OMS-2 in the presence of 2-aminopyridine for 2 h at 100 °C. Then, HOAc was added into the mixture and the reaction was run for 20 h again under air. In this way, this one-pot synthesis gave the corresponding 3-aroylimidazo[1,2-*a*]pyridines in 52-75% yields without using any additives (Scheme 3).

**Table 4** The recyclability of Cu/H-OMS-2[a]

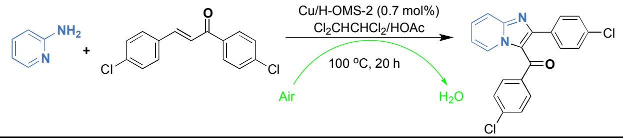

| Run | 1 | 2 | 3 | 4 | 5 |
|---|---|---|---|---|---|
| Isolated yield (%) | 82 | 78 | 70 | 65 | 48 |

[a] Reaction conditions: 2-aminopyridine (0.6 mmol), chalcone (0.4 mmol), Cu/H-OMS-2 (12 mg, 0.7 mol%), $Cl_2CHCHCl_2$ (1.2 mL), HOAc (0.1 mL), 100 °C, 20 h, air.

Finally, recovery and recyclability of the heterogeneous catalyst were studied by the reaction between 2-aminopyridine and 4,4`-dichlorochalcone using 0.7 mol% of Cu/H-OMS-2 in the mixed solvent at 100 °C for 20 h under air. After each run, Cu/H-OMS-2 was easily isolated by centrifugation, then washed by water and finally dried at 110 °C for the next experiment. The image of TEM demonstrated that the morphology of the used Cu/H-OMS-2 is not changed and it is stable on structure (see SI, Figure S4). The experimental results showed that Cu/H-OMS-2 could be reutilized four times with an increasing decrease in the catalytic activity and the activity of the catalyst significantly dropped to 48% after four runs (Table 4). After the first run, inductively coupled plasma-atomic emission spectroscopy (ICP-AES) was used to analyze the reaction solution after filtration of the catalyst, which showed 0.5 ppm of copper leached from Cu/H-OMS-2. The leached copper from the catalyst perhaps incurs the loss of the catalytic activity. Furthermore, a hot filtration experiment (for experiment detail, see SI, Scheme S1) showed the leached copper species in the solution is catalytically inactive and cannot trigger the reaction at all. Therefore, it is believed that the observed catalysis is derived from the solid catalyst rather than the leached copper species, and the catalyst is heterogeneous in nature.

## Conclusions

In conclusion, we have employed Cu/H-OMS-2 as an efficient catalyst in the heterogeneous biomimetic oxidative synthesis of 3-aroylimidazo[1,2-*a*]pyridines and 3-aroylimidazo[1,2-*a*]pyrimidines. The reactions proceed in a mixed solvent of $Cl_2CHCHCl_2$ and HOAc in the presence of a very low amount of catalyst (Cu: 0.7 mol%) and air as the oxidant without the use of bases and ligands. Moreover, the catalyst can also be applied in one-pot reaction of ketone, aldehyde and 2-aminopyridine. More importantly, the results from $H_2$-TPR prove that the redox ability of Cu/H-OMS-2 is significantly improved because of the electronic interaction between Cu and H-OMS-2. For the catalyst, the low loading Cu plays a role of catalytic metal and H-OMS-2 is used as an ETM as well as an excellent support, which sequentially decreases the redox energy barrier during the oxidative transformation to make the electrons transfer rapidly. Finally, the highly dispersed Cu/H-OMS-2 is natural heterogeneous and recyclable.

## Experimental Section

Unless otherwise noted, all reagents were purchased from commercial suppliers and used without further purification. Metal salts were commercially available and were used directly. All experiments were carried out under air. Flash chromatography was carried out with Merck silica gel 60 (200-300 mesh). Analytical TLC was performed with Merck silica gel 60 F254 plates, and the products were visualized by UV detection. $^1H$ NMR and $^{13}C$ NMR (400 and 100 MHz respectively) spectra were recorded in $CDCl_3$. Chemical shifts ($\delta$) are reported in ppm using TMS as internal standard, and spin-spin coupling constants ($J$) are given in Hz. Cu/OMS-2[9a] (2.0 wt.% theoretical loading, actual loading is 1.65 wt.%) was synthesized by wet impregnation in deionized water and $Cu(OH)_x$/OMS-2[9b] (2.0 wt.% theoretical loading, actual loading is 1.45 wt.%) was made by deposition-precipitation in water.

### Catalyst characterization methods

The crystal phase and composition of catalysts were determined by power X-ray diffraction using a X-Pert PRO X-ray diffractometer with Cu Ka radiation in the 2θ ranges of 10–90°. Infrared spectra of the materials were recorded on calcined powders dispersed in KBr (2 mg sample in 300 mg KBr) using a Perkin-Elmer One FTIR spectrometer with a resolution of 4 $cm^{-1}$ operating in the range 500-2000 $cm^{-1}$ with 4 scans per spectrum. The morphologies of the samples were characterized by a TF20 transmission electron microscope and SM-5600LV scanning electron microscope. Nitrogen adsorption-desorption measurements were performed at 76 K using an ASAP 2020M analyzer utilizing the BET model for the calculation of specific surface areas. The reducibility of the catalysts was measured by the hydrogen temperature-programmed reduction ($H_2$-TPR) technique. A 50 mg of OMS-2, H-OMS-2 or Cu/H-OMS-2 was placed in a quartz reactor that was connected to a TPR apparatus and the reactor was heated from r.t. to 550 $^oC$ with a heating rate of 10 $^oC$/min. The reducing atmosphere was the mixture of $H_2$ and $N_2$ with a total flow rate of 30 mL/min and the amount of $H_2$ uptake during the reduction was measured by a thermal conductivity detector (TCD). The oxygen species of the catalysts was investigated by the oxygen temperature-programmed desorption ($O_2$-TPD) technique. A 50 mg of H-OMS-2 or Cu/H-OMS-2 was place in a quartz reactor that was connected to a TPD apparatus and the reactor was purged with He at room temperature for 1 h followed by heating to 950 $^oC$ at 10 $^oC$/min in the same atmosphere.

#### Preparation of H-OMS-2[4c]

H-OMS-2 was synthesized by ion-exchange with homemade OMS-2. The concentrated $HNO_3$ (50 mL) was added to OMS-2 (2 g) and the slurry was stirred vigorously at 80 $^oC$ for 6 h. The product was filtered and washed by deionized water for many times. Then, the product was dried at 120 $^oC$ for 12 h in an oven and calcined at 280 $^oC$ for 6 h.

#### Preparation of Cu/H-OMS-2

Support H-OMS-2 (2 g) was added to a 50 mL round-bottom flask. A solution of $Cu(NO_3)_2 \cdot 3H_2O$ (0.15 g) in deionized water (10 mL) was added to H-OMS-2, and additional deionized water (10 mL) was added to wash down the sides of the flask. Then the flask was submerged into an ultrasound bath for 3 h at room temperature and stirred for further 20 h at room temperature. After that, the water was distilled under reduced pressure on a rotary evaporator at 80 $^oC$ for more than 2 h. Finally, the black powder was dried into an oven at 110 $^oC$ for 4 h followed by calcination at 350 $^oC$ under air for 2 h. The black powder Cu/OMS-2 (2.0 wt.% theoretical loading, actual loading is 1.58 wt.%) was characterized by ICP-OES, BET, XRD, XPS, FTIR, TEM, SEM, $H_2$-TPR and $O_2$-TPD techniques.

#### General procedure for Cu/H-OMS-2-catalyzed 3-aroylimidazo[1,2-a]pyridines synthesis

Cu/H-OMS-2 (12 mg, 0.7 mol%), 2-aminopyridine (0.6 mmol), chalcones (0.4 mmol) and $Cl_2CHCHCl_2$ (1.2 mL)/HOAc (0.1 mL) were added to a flask with a bar. The flask was stirred at 100 $^oC$ for 20 h under air. After cooling to room temperature, the mixture was diluted with ethyl acetate and filtered. The filtrate was removed under reduced pressure to get the crude product, which was further purified by silica gel chromatography (petroleum/ethyl acetate = 4/1 as eluent) to yield corresponding product. The identity and purity of the products was confirmed by $^1H$ and $^{13}C$ NMR spectroscopic analysis.

## Acknowledgements

We gratefully acknowledge the National Natural Science Foundation of China (Grant Nos. 21403256, 21573261, 21372102) and the Suzhou Industrial Technology and Innovation Project (Grant No. SYG201531).

## Notes and references

1 (a) S. L. Suib, *Acc. Chem. Res*. 2008, **41**, 479-487; (b) S. L. Suib, *J. Mater. Chem*. 2008, **18**, 1623-1631; (c) Y. F. Shen, R. P. Zerger, R. N. DeGuzman, S. L. Suib, L. McCurdy, D. I. Potter and C. L. O΄Young, *Science,* 1993, **260**, 511-515..

2 (a) R. N. DeGuzman, Y.-F. Shen, E. J. Neth, S. L. Suib, C.-L. O΄Young, S. Levine and J. M. Newsam, *Chem. Mater.,* 1994, **1**, 815-821; (b) Y. C. Son, V. D. Makwana, A. R. Howell and S. L. Suib, *Angew. Chem. Int. Ed*., 2001, **40**, 4280-4283; (c) R. Ghosh, X. Shen, J. C. Villegas, Y. Ding, K. Malinger and S. L. Suib, *J. Phys. Chem. B,* 2006, **110**, 7592-7599.

3 (a) K. Yamaguchi, Y. Wang and N. Mizuno, *ChemCatChem,* 2013, **5***,* 2835-2838; (b) K. Yamaguchi, H. Kobayashi, Y. Wang, T. Oishi, Y. Ogasawara and N. Mizuno, *Catal. Sci. Technol*., 2013, **3**, 318-327; (c) Y. Wang, H. Kobayashi, K. Yamaguchi and N. Mizuno, *Chem. Commun*., 2012, **48**, 2642-2644; (d) K. Yamaguchi, H. Kobayashi, T. Oishi and N. Mizuno, *Angew. Chem. Int. Ed.,* 2012, **51**, 544-547; (e) X. Meng, J. Zhang, G. Chen, B. Chen and P. Zhao, *Catal. Comm*., 2015, **69**, 239–242; (f) X. Jin, K. Yamaguchi and N. Mizuno, *RSC Adv.,* 2014, **4***,* 34712-34715.

4 For the selected papers on the application of modified OMS-2 in oxidations, see: (a) R. Kumar, S. Sithambaram and S. L. Suib, *J. Catal.,* 2009, **262**, 304-313; (b) X. Chen, Y. Shen, S. L. Suib and C. L. O'Young, *Chem. Mater*., 2002, **14**, 940-948; (c) V. P. Santos, O. S. G. P. Soares, J. J. W. Bakker, M. F. R. Pereira, J. J. M. Órfão, J. Gascon, F. Kapteijn and J. L. Figueiredo, *J. Catal.,* 2012, **293**, 165-174; (d) S. Sithambaram, R. Kumar, Y.-C. Son and S. L. Suib, *J. Catal.,* 2008, **253**, 269–277; (e) Y.-G. Yin, W.-Q. Xu and S. L. Suib, I*norg. Chem*., 1995, **34**, 4187-4193.

5 (a) X.-S. Liu, Z.-N. Jin, J.-Q. Lu, X.-X. Wang and M.-F. Luo, *Chem. Eng. J*., 2010, **162**, 151-157; (b) W. Y. Hernándeza, M. A. Centeno, S. Ivanova, P. Eloy, E. M. Gaigneaux and J. A. Odriozola, *Appl. Catal. B: Environ.,* 2012, **123**, 27-35; (c) M. Özacara, A. S. Poyraz, H. C. Genuino, C.-H. Kuo, Y. Meng and S. L. Suib, *Appl. Catal. A: Gen*., 2013, **462**, 64-74.

6 M. Sun, L. Yu, F. Ye, G. Diao, Q. Yu, Z. Hao, Y. Zheng and L. Yuan, *Chem. Eng. J.,* 2013, **220**, 320-327.

7 Y. Yang, J. Huang, S. Zhang, S. Wang, S. Deng, B. Wang and G. Yu, *Appl. Catal. B: Environ.,* 2014, **150**, 167-178.

8 For the selected papers on the application of ETMs in homogeneous catalysis, see: (a) J. Piera and J. E. Bäckvall, *Angew. Chem. Int. Ed*., 2008, **47**, 3506-3523; (b) B. P. Babu, X. Meng and J. E. Bäckvall, *Chem. Eur. J.,* 2013, **19**, 4140-4145; (c) Y. Endo and J. E. Bäckvall, *Chem. Eur. J.,* 2012, **18**, 13609-13613; (d) X. Meng, C. Li, B. Han, T. Wang and B. Chen, *Tetrahedron,* 2010, **66**, 4029-4013; (e) N. Gigant and J. E. Bäckvall, *Org. Lett.,* 2014, **16**, 1664-1667; (f) N. Gigant and J. E. Bäckvall, *Org. Lett.,* 2014, **16**, 4432-4435; (g) N. Gigant and J. E. Bäckvall, *Chem. Eur. J.,* 2013, **19**, 10799-10803.

9 (a) X. Meng, C. Yu, G. Chen and P. Zhao, *Catal. Sci. Technol*., 2015, **5**, 372-379; (b) T. Oishi, K. Yamaguchi and N. Mizuno, *ACS Catal.,* 2011, **1**, 1351-1354.

10 (a) J. C. Teulade, G. Grassy, J. P. Girard and J. P. Chapat, *Eur. J. Med. Chem.,* 1978, **13**, 271-276; (b) A. Gueiffier, M. Lhassani, A. Elhakmaoui, R. Snoeck, G. Andrei, O. Chaxignon, J. C. Teulade, A. Kerbal, E. M. Essassi, J. C. Debouzy, M. Witvrouw, Y. Blache, J. Balzarini, E. De Clercq and J. P. Chapat, *J. Med. Chem.,* 1996, **39**, 2856-2859; (c) M. Hranjec, I. Piantanida, M. Kralj, L. Suman, K. Pavelić and G. Karminski-Zamola, *J. Med. Chem.,* 2008, **51**, 4899-4910; (d) C.

Hamdouchi, J. De Blas, M. del Prado, J. Gruber, B. A. Heinz and L. Vance, *J. Med. Chem.,* 1999, **42**, 50-59.
11 M. Baumann, I. R. Baxendale, S. V. Ley and N. Nikbin, *Beilstein J. Org. Chem.,* 2001, **7**, 442-495.
12 (a) Y.-S. Tung, M. S. Coumar, Y.-S. Wu, H.-Y. Shiao, J.-Y. Chang, J.-P. Liou, P. Shukla, C.-W. Chang, C.-Y. Chang, C.-C. Kuo, T.-K. Yeh, C.-Y. Lin, J.-S. Wu, S.-Y. Wu, C.-C. Liao and H.-P. Hsieh, *J. Med. Chem*., 2011, **54**, 3076-3080; (b) H.-P. Hsieh, Y.-S. Chao, J.-P. Liou, J.-Y. Chang and Y.-S. Tung, Antitumor compounds. US7456289, 2008.
13 (a) K. Monir, A. K. Bagdi, S. Mishra, A. Majee and A. Hajra, *Adv. Synth. Catal.,* 2014, **356**, 1105-1112; (b) P. Kaswan, K. Pericherla, H. K. Saini and A. Kumar, *RSC Adv*., 2015, **5**, 3670-3677; (c) P. Kaswan, K. Pericherla, Rajnikant and A. Kumar, *Tetrahedron,* 2014, **70**, 8539-8544; (d) K. R. Reddy, A. S. Reddy, R. Shankar, R. Kant and P. Das, *Asian J. Org. Chem.,* 2015, **4**. 537-583.
14 S. Goswami, S. Jana, A. Hazra and A. K. J. Adak, *Heterocycl. Chem*., 2007, **44**, 1191-1194.
15 For selected examples of heterogeneous catalytic organic synthesis, see: (a) K. Natte, H. Neumann and X.-F. Wu, *Catal. Sci. Technol*., 2015, **5**, 4474-4480; (b) X. Meng, X. Xu, T. Gao and B. Chen, *Eur. J. Org. Chem.,* 2010, 5409-5414; (c) A. T. Nguyen, L. T. Pham, N. T. S. Phan and T. Truong, *Catal. Sci. Technol*., 2014, **4**, 4281-4288; (d) X. Meng, Y. Wang, C. Yu and P. Zhao, *RSC Adv.,* 2014, **4**, 27301-27307; (e) X. Meng, C. Yu and P. Zhao, *RSC Adv.,* 2014, **4**, 8612-8616; (f) J. Chen, L He, K. Natte, H. Neumann, M. Beller and X.-F. Wu, *Adv. Synth. Catal*., 2014, **356**, 2955-2959.
16 M. Ousmane, G. Perrussel, Z. Yan, J.-M. Clacens, F. De Campo and M. Pera-Titus, *J. Catal*., 2014, **309**. 439-452.
17 V. P. Santos, M. F. R. Pereira, J. J. M. Órfão and J. L. Figueiredo, *Appl. Catal. B: Environ*., 2010, **99**, 353-363.
18 (a) S. V. Ley and A. W. Thomas，*Angew. Chem. Int. Ed.,* 2003, **42**, 5400-5449; (b) C. C. C. J. Seechurn, M. O. Kitching, T. J. Colacot and V. Snieckus, *Angew. Chem. Int. Ed*., 2012, **51**, 5062-5085.

# Graphic Abstract

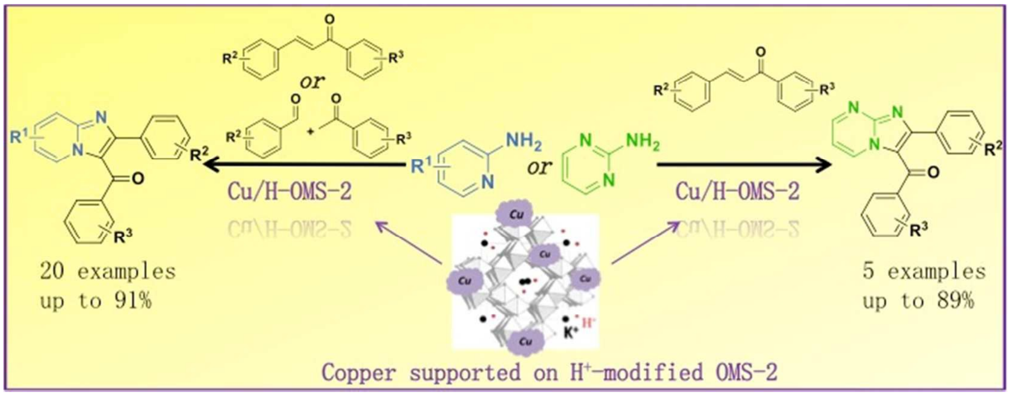

The combination of Cu and H-OMS-2 is employed to synthesize heterocycles through multistep oxidation under a low-energy pathway.